UNIVERSITI SAINS MALAYSIA

Laporan Akhir Projek Penyelidikan Jangka Pendek

Development of Nanocrystalline Ferroelectric PLZT Powder by a Modified Coprecipitation Method

by

Prof. Dr. Radzali Othman

Dr. Yeoh Fei-Yee

Assoc. Pror. Dr. Azizan Aziz

2008

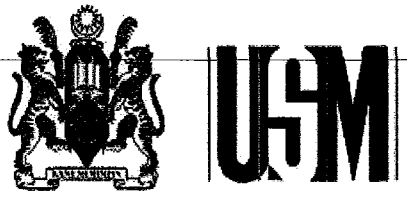

UNIVERSITI SAINS MALAYSIA

END OF PROJECT REPORT

Development of Nanocrystalline Ferroelectric PLZT Powder by a Modified Coprecipitation Method

(A Project Supported By A Grant From The Nippon Sheet Glass Foundation)

Radzali OTHMAN
Fei-Yee YEOH
Azizan AZIZ

School of Materials & Mineral Resources Engineering
Universiti Sains Malaysia

2008

END OF PROJECT REPORT

Development of Nanocrystalline Ferroelectric PLZT Powder
by a Modified Coprecipitation Method

Radzali Othman & Associates
radzali@eng.usm.my

Abstract

This research was focused on producing nanocrystalline ferroelectric lead lanthanum zirconate titanate or more commonly known as PLZT. A modified coprecipitation technique was used in this study to produce the nanocrystalline PLZT powder. The calcination temperatures were varied so as to obtain the optimum temperature to form the desired perovskite structure. The powder so produced was then pressed into pellets and sintered at different temperatures to obtain densified pellets. The pellets were then examined for microstructure and electrical properties (emphasis on dielectric behaviour) to determine enhancement in properties of the nanocrystalline PLZT.

Introduction

Ferroelectric PLZT is an important electronic and optoelectronic material. It can be used as materials for memory devices, piezoelectric actuators, optical modulators, and capacitors. Sometimes, as a ferroelectric material, it is also referred as a smart material due to its capability of being used both as sensors and actuators. The PLZT can be produced in different forms for different applications, viz as powders for capacitors, as thin films for memory materials, as thick films for piezoelectric devices, and as fibers for optical devices. Recent advances in technology have enabled miniaturization which is important to reduce the production cost, enhance product features and improve materials performance. Thus, nano PLZT powders come into prominence with the principle objective to reduce the size of capacitors and hence minimize production cost. Phase morphology and characteristics of PLZT ceramic powder highly depend on their method of preparation. As with any other ceramic materials, PLZT is conventionally synthesized from mixed oxide or solid state reactions. Although having the advantages of cost effectiveness and being a simpler process, its high calcination temperature, impurities induced during processing, and products with chemical inhomogeneities had led to attempts to find alternative routes. Thus, several alternative routes such as sol-gel,

coprecipitation, hydrothermal, Pechini's, and partial oxalate methods had been developed to cater for different needs. Among all the methods, coprecipitation has been reported as a prominent synthesis method in producing high-purity PLZT product. In the present work, 3 coprecipitation methods had been carried out to produce PLZT powders. The method which produced the most desirable PLZT powder (based on XRD results) was then selected for further work.

Materials & Experimental Methods

Method 1 – Oxalate coprecipitation

Water soluble starting chemicals such as lead nitrate ($Pb(NO_3)_2$, Fluka, Switzerland), lanthanum chloride hydrate ($LaCl_3$·aq, Fluka, Switzerland), zirconium oxynitrate ($ZrONO_3$, Riedel-de-Haën, Germany), potassium titanyl oxalate ($K_2TiC_4O_9 \cdot 2H_2O$, Fluka, Switzerland) were dissolved in water, respectively. Lanthanum chloride aqueous solution was added into lead nitrate aqueous solution to obtain a PL solution. ZT solution was prepared with the same procedure. PL solution was then dripped into ZT solution to obtain a precipitate. The precipitate was collected with a Millipore filter system and dried in an oven at 100°C for 8 hours. The precipitate was then filtered and dried to form a precursor powder A.

Method 1

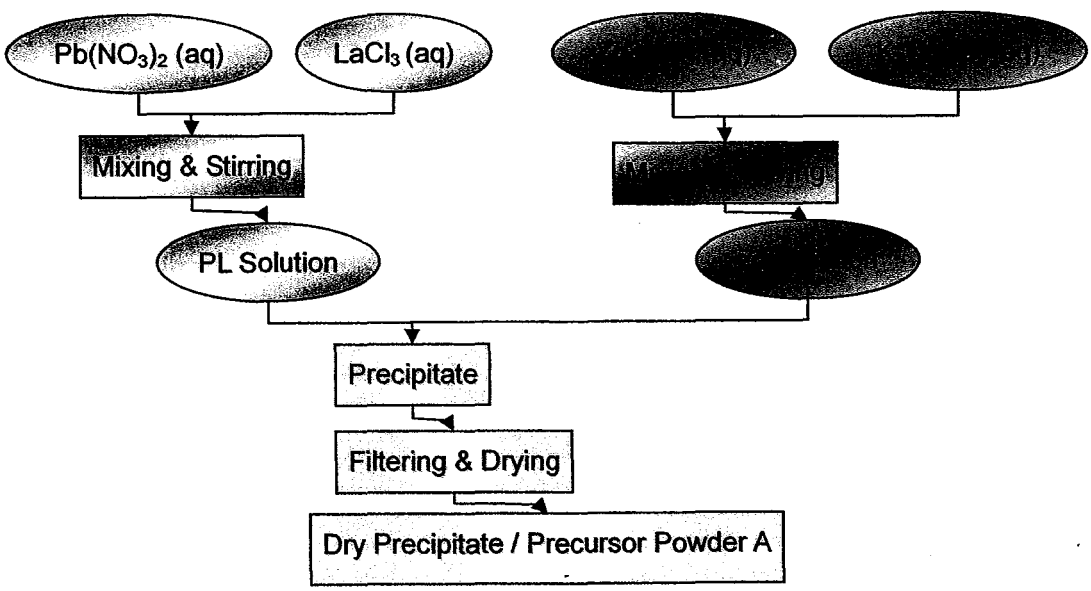

Method 2 – Organometallic coprecipitation

PL solution was prepared according to the same procedure as in method 1. Zirconium (IV) propoxide ($ZrC_{12}H_{28}O_4$, Fluka, Switzerland) and tetraisopropyl orthotitanate ($TiC_{12}H_{28}O_4$, Fluka, Switzerland) were stabilized with triethanolamine, or in short TEA, ($N(CH_2{\cdot}CH_2{\cdot}OH)_3$, BDH, England), respectively. Both stabilized solutions were mixed to obtain a ZT solution. ZT solution was again dripped into PL solution to form a precipitate before the powder was filtered and dried. The powder obtained from this method is named as precursor powder B.

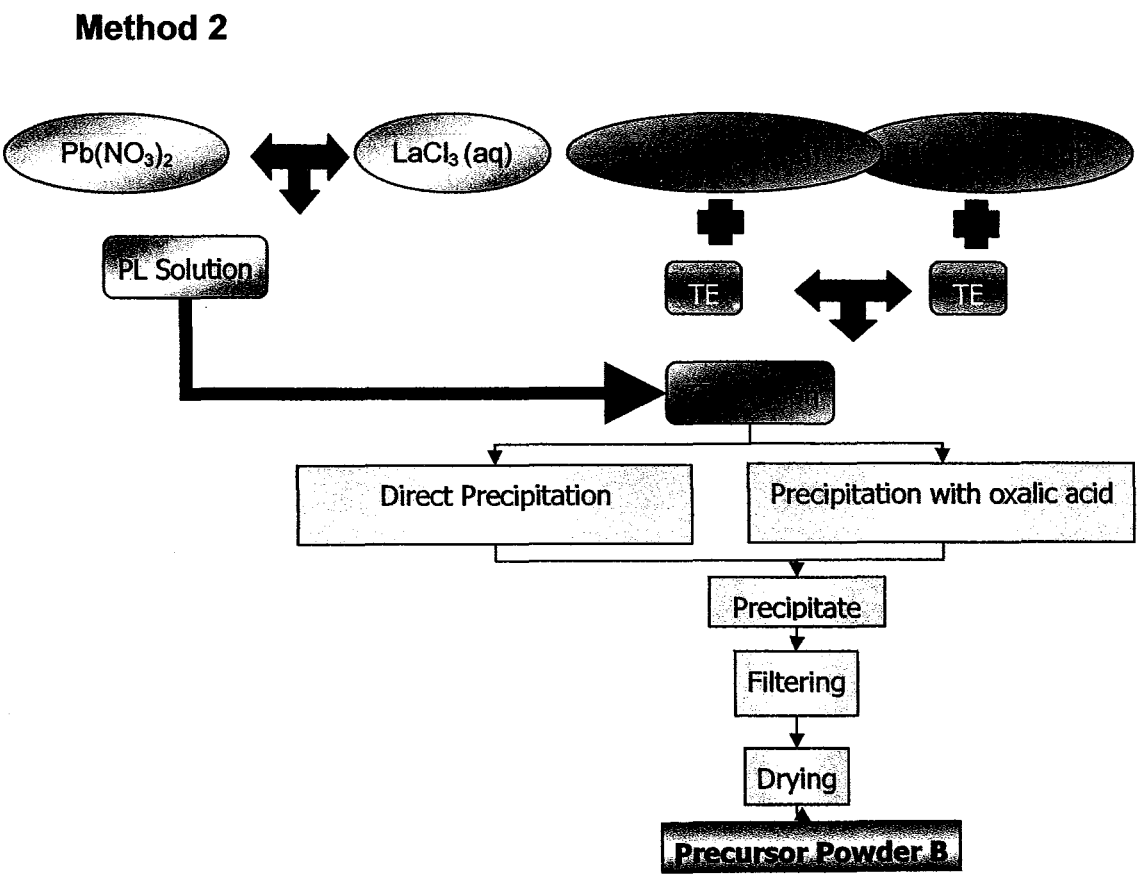

Method 3 – Hydroxide coprecipitation

Aqueous lead nitrate solution was prepared as above. Lanthanum oxide (La_2O_3, Fluka, Switzerland), was dissolved in nitric acid (HNO_3, Merck, Germany). Both solutions were mixed to obtained a PL solution. Zirconium oxychloride octahydrate ($ZrOCl_2 \cdot 8H_2O$, Fluka, Switzerland) and tetraethyl orthotitanate ($TiC_8H_{20}O_4$, Merck, Germany) were precipitated in ammonia solution (NH_3, BDH, England) and filtered respectively. The respective precipitates were dried and ground into fine powder before it was dissolved in nitric acid. Both solutions were mixed to obtain ZT solution. PL solution was finally dripped into ZT solution to yield a precipitate. The precipitate was then dried and ground into precursor powder C.

Method 3

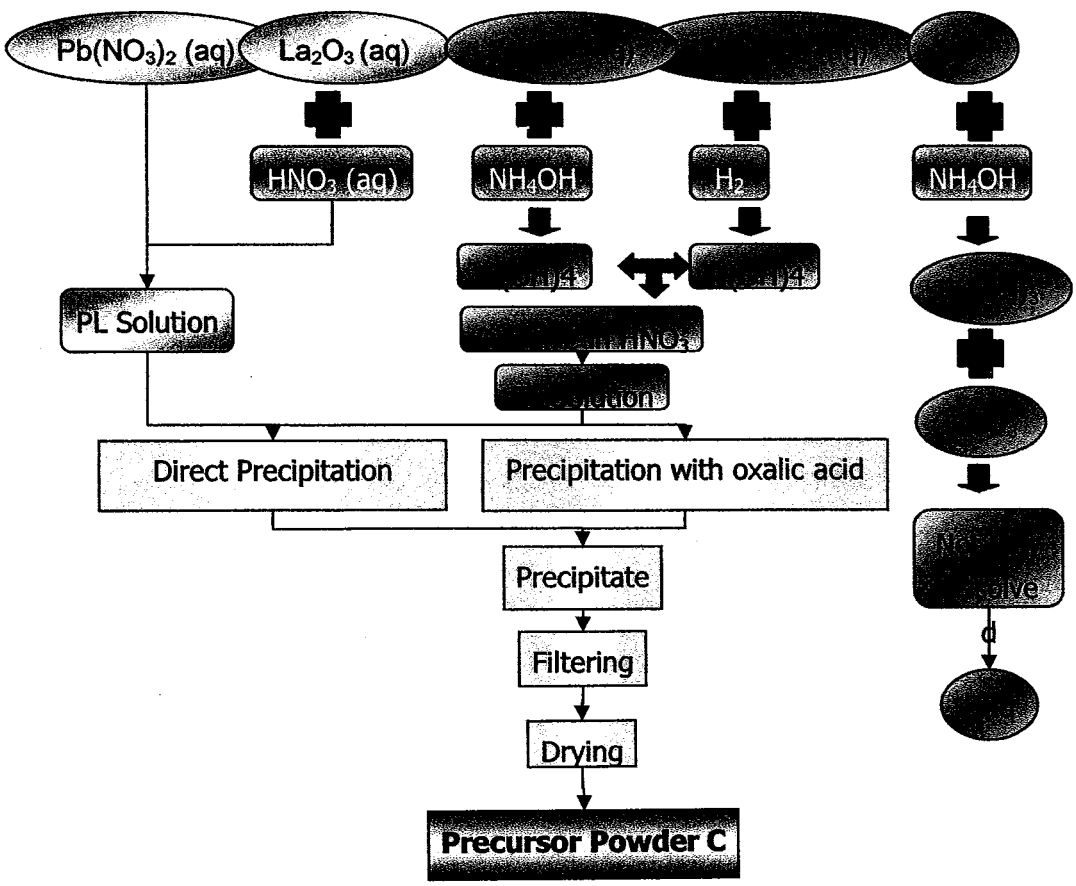

All the precursor powders produced from the respective methods were examined with XRD. Calcination temperature for each precursor powder was optimized using thermal analysis TG-DSC (except powder from method 3). The phase of each calcined powder was then checked with XRD again for phase identification. Estimated spherical diameter (ESD) of the particle (for powder produced from the selected method) was calculated from the surface area measured from a BET method. The size and shape of the powder were observed under a SEM and a TEM.

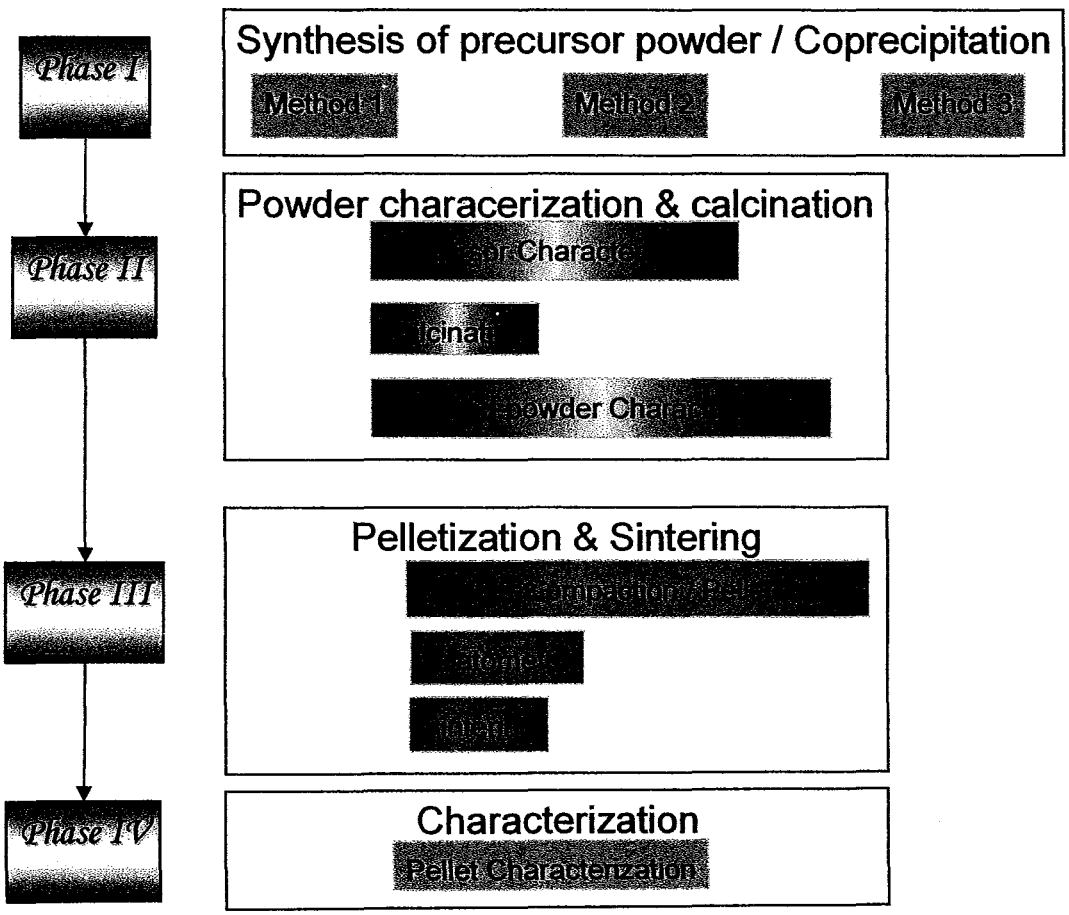

Results and Discussion

The precursor powder produced from each method was examined with XRD. The diffractograms obtained from the XRD are shown below. Figure 1 shows that some $PbTiO_3$ or PT peaks (ICDD 40-99 and ICDD 11-0193) were detected on top of the amorphous phase. These peaks show PT phase was formed during the precipitation even before the powder was calcined. Figures 2 and 3 show that both the precursor powders B and C contain more homogeneous phase compared to precursor powder A. No crystalline peak was observed from the diffractograms which disclose the amorphous nature of the phase in the precursor powders.

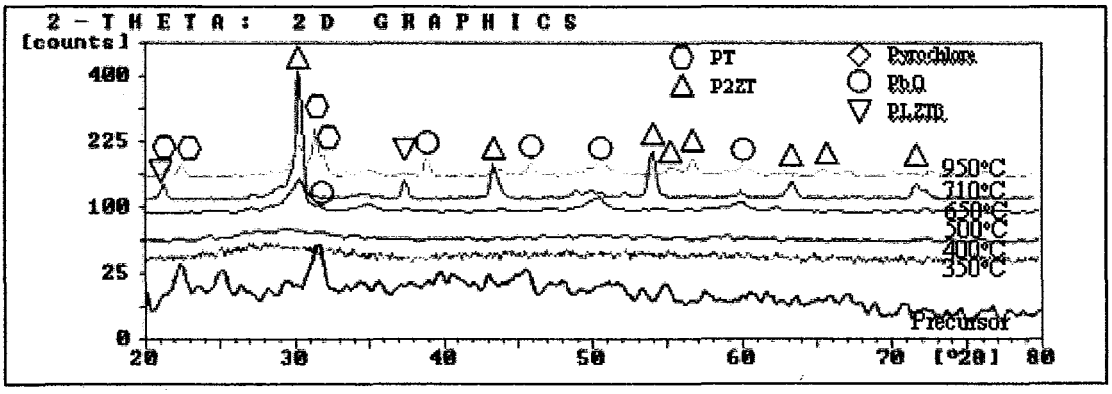

Figure 1. XRD diagram for sample A obtained by method 1

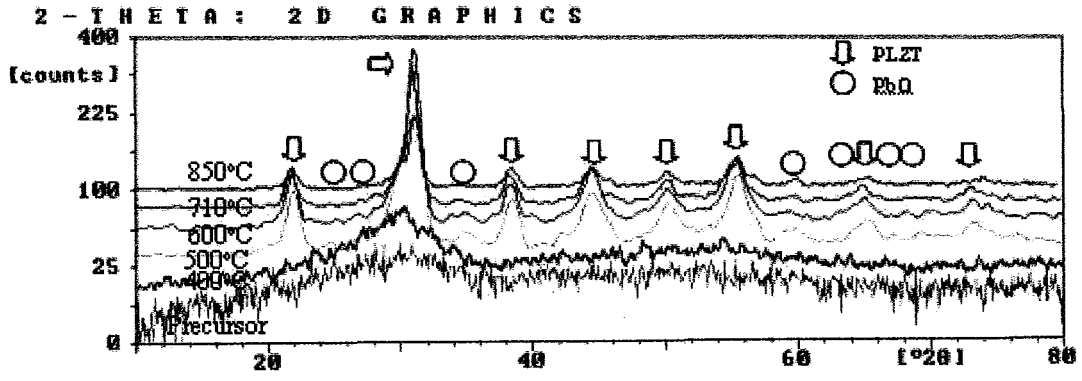

Figure 2. XRD diagram for sample B obtained by method 2

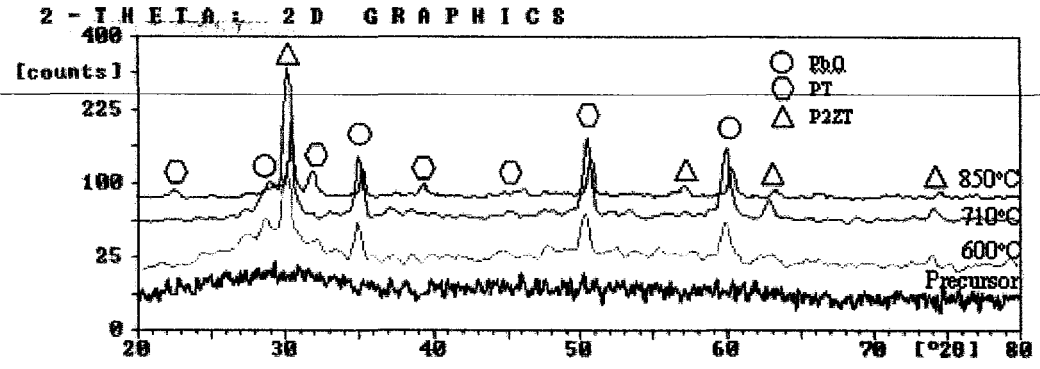

Figure 3. XRD diagram for sample C obtained by method 3

The precursor powders were next analyzed with a simultaneous differential scanning calorimetry (DSC) and thermal gravimetry analysis (TGA). Due to the limited access of the facility, only precursor powder A and B were tested. The thermograms (TG-DSC) for the precursor powder A are shown in Figure 4 whilst the TG-DSC results for precursor powder B are shown in Figure 5. Figure 4 shows the mass change and enthalpy change activities of sample precursor powder A. Up to ≈280 °C, 2 minor weight losses of 4.3 % and 5.7 % with respective peaks at 91 °C and 189 °C are detected in an endothermic effect of 318.4 J/g. This effect was due to the evaporation of surface moisture. Two exothermic peaks at 341.86 °C and 383.65 °C were found in a major exothermic effect of -710.5 J/g. At the same region in the TG curve, 2 major weight losses (16.388 % and 5.212 %) at 340 °C and 430 °C are detected in line with the 2 major exothermic peaks mentioned above. The former weight loss is attributed to changes of chemical structure of the amorphous phase in the powder. This can be proven from the XRD diffractograms (Figures 1, 2, 3) where no crystalline peaks are observed for powders calcined within this range of temperatures. The latter is related to the decomposition of organic compounds present in the precipitate as reported by Potdar et al. (1994) on the decomposition of oxalate compounds at 300-400 °C. It is believed that the crystallization process of sample A takes place at a temperature around 600-700 °C where a small weight loss of 2.9 % and an exothermic effect of 17.1 J/g (peak at 643.18 °C) were found. The next exotherm of 41.7 J/g was detected at 864.68 °C without any mass change involved and can most probably be attributed to enthalpy change during a phase transition. Toward the end of the test, a continuous mass loss of 15.7 % begun at temperature around 900 °C. This mass loss, with an endothermic peak (148.7 J/g) at 1325.43 °C, is believed to be caused by the evaporation of volatile lead oxide in the powder.

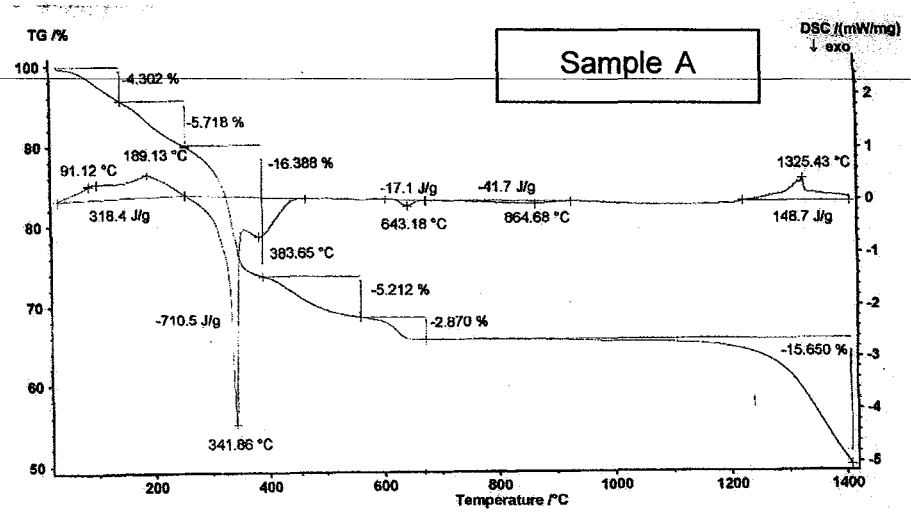

Figure 4 TG-DSC thermogram for Sample A

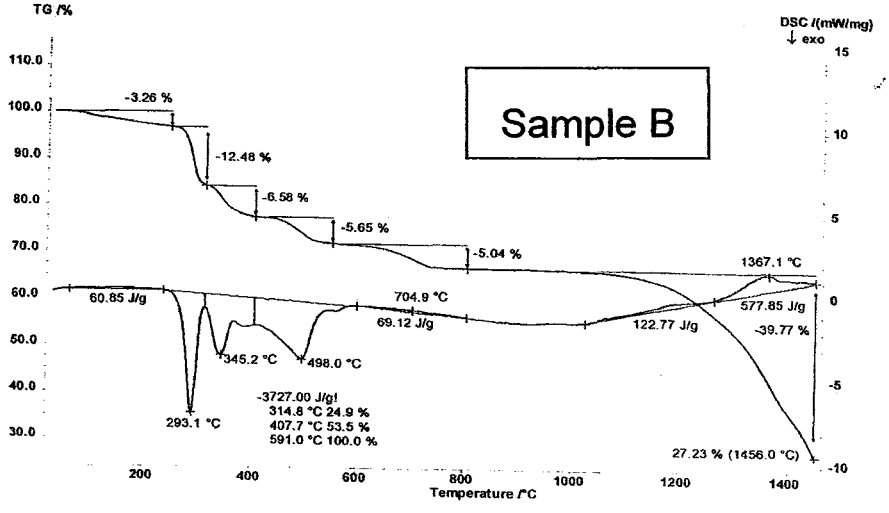

Figure 5. TG-DSC thermogram for Sample B

From the thermogram shown in Figure 5, a total of 3.3 % mass loss and an endotherm of 60.85 J/g were found up to 200 °C. This event is attributed to the liberation of surface-adsorbed water which took place at the same region for all the samples. A sharp exothermic peak is observed at 293.1 °C starting at around 200 °C with a major mass loss at 291 °C. This sharp peak indicates a large amount of heat is released concurrently with a mass loss in a short period of time. It is most probably due to the oxidative decomposition of the organic compound TEA which is supposed to start decomposing at a temperature of 200 °C (Das et al., 1998).

2 successive broad exothermic peaks at 345.2°C and 498.0°C (with 2 mass loss of about 5-6 %) thereafter indicate that organic decomposition is not completed at 290°C. The first enthalpy change and mass loss at a temperature around 345°C could be due to the decomposition of the remaining alkoxide compounds contributed by zirconium propoxide and tetraethyl orthotitanate respectively, or a combination of alkoxide and TEA compounds. The primary organic source (TEA and isopropoxide) could be decomposed into another form of secondary organic compound(s), for instance, carbonate group. Yang (2001) pointed out that acetate group decomposed into carbonate at 300°C. This secondary organic compound(s) could be further decomposed at a higher temperature. Similar phenomenon could be found in this situation where the exothermic peak and mass loss at a temperature of around 498.0 °C which can be due to the decomposition of secondary organic compound(s) or carbon residue(s). As a consequence from the decomposition of multi organic components, continuous exotherms with multi peaks at 345.2 and 498.0 °C, which overlapped with each other, are detected. The dark brown colour of the powder calcined at 400 °C leads to a suspicion of high carbon content in the powder. This was also pointedout in the literature (Saha & Pramanik, 1997) which stated the oxidative decomposition of organic compound present is in the range of 330-455 °C.

A small endothermic peak which is observed around 704.9 °C corresponds to the phase change of a crystal structure. In combination with the observation of the colour of calcined powders, the yellow colour of the powder calcined at 500°C onwards indicates the presence of lead oxide. This also gives an idea that the formation of a PLZT structure occurs around 500-700 °C. The peaks of these thermal activities were not spotted from the thermograms mainly due to the overlapping of the low intensity crystallization peak with the broad organic decomposition peak at the same range of temperatures. As a result, the crystallization peak cannot be detected from the thermogram. However, the volatile PbO evaporate at a higher temperature starting at 1000 °C compared to 900 °C in the precursor powder A although the endothermic peak with a mass loss of 39.77 % was found at the same temperatures of about 1300 °C. This might indicate that the phase of PLZT produced with this method is much more stable and temperature-resistant compared to all previous methods.

For simplicity, calcination temperatures of precursor powders were predicted from the existing thermograms for other samples. From the previous thermograms, the organic decomposition will only be completed at temperatures higher than 500 °C. Thus, the

calcination temperature for precursor powder C was predicted to be 600 and 710 °C which is the temperatures below and above a minor peak, suspected to be a crystallization peak. It is also calcined at the highest temperature of 850 °C since a small peak is detected at this range of temperature for sample A. Table 1 summarizes the enthalpy change and mass loss of precursor powders A and B.

Table 1: Summary of TG-DSC results for precursor powders A and B

Temperature	Sample A	Sample B
100-200°C	Moisture Removal	Moisture Removal
200-600°C	Organic Decomposition	Organic Decomposition Phase Formation
600-800°C	Phase Transition	Phase Transition
800-850°C	Phase Transition	-
➢ 900°C	PbO Evaporation	PbO Evaporation

Precursor powder A which was obtained by Method 1 (oxalate coprecipitation) was calcined according to the peaks obtained from TG-DSC thermogram. From the thermogram, there are 2 major peaks at 343.2 °C and 436.3 °C. According to the assumption made in TG-DSC analysis, these peaks refer to the decomposition of organic compounds. There is a possibility that a crystal formation peak could be overlapped by these 2 large peaks. Therefore, precursor powder A was calcined in this range of temperature as well, i.e. 350, 400, and 500 °C.

The X-ray diffractogram shows that the precursor powder A (Figure 1) synthesized with Method 1 consists of a small amount of crystalline $PbTiO_3$ (PT) within an amorphous matrix. This PT peak disappears as the powder was calcined at 350 -500 °C, where only an amorphous structure is observed. This agrees with the assumption which has been made earlier in the TG-DSC discussion that there is almost no crystalline peak until 500 °C. It confirms that there is no crystalline phase formation associated with the 343.2 and 436.3 °C TG-DSC peaks as suspected prior to this. As the temperature increases to 650 °C, $Pb_2(ZrTi)O_3$ peak (abbreviated as P2ZT – ICDD 14-31) starts to appear which is confirmed by the peak 643.18°C in the TG-DSC thermogram. The crystallization of P2ZT is optimised at a temperature around 710 °C, as shown by the diffractogram in Figure 1. Minor peaks which correspond to β-$Pb_{1-x}La_x(Zr_{8.27x}Ti_z)_{1-0.25x}O_3$ (abbreviated as βPLZT) phase (ICDD 29-776) are observed at this temperature. This indicates that the

powder calcined at this temperature also do not produce a pure P2ZT. As the sample was calcined to a higher temperature (850°C), the intensity for P2ZT peaks becomes lower. More peaks corresponding to $PbTiO_3$ (ICDD 6-0452) and $3PbO{\cdot}nH_2O$ (ICDD 22-1134) appear showing that loss of lead from the sample occurs via a specific mechanism. The PbO diffuses from the P2ZT structure and this leads to the breakdown of the P2ZT structure. Remaining elements formed a new structure PT without Zr. The β-PLZT seems to disappear completely and there seems not to be any crystalline phase with La. None of the La compound exists in any diffractogram above. There is no sign of La_2O_3. This indicates the failure of La to be incorporated into the crystalline structure without a complexing agent. It is believed that La remains in solution or within an amorphous phase. As a conclusion, this method is not effective in producing PLZT structure.

Figure 2 show that the precursor powder produced by the organic coprecipitation method is amorphous in nature as mentioned. The powder maintains its amorphous nature even after calcination up to 400 °C. After being calcined at 500°C, PLZT peaks start to appear accompanied by some possible minor $3PbO{\cdot}nH_2O$ peaks. The most intense set of peaks are observed when the precursor powder B was calcined at 500 °C. No crystallization peak is observed in the TG-DSC thermogram in Figure 2, but only a broad peak of organic decomposition. It can be concluded that the thermal crystallization peak which took place at this temperature was camouflaged under the organic decomposition peak. The calcination temperatures in the literature, which also use a wet chemical synthesis method, revealed values of 800°C by Choy & Han (1997), 700°C by Cerqueira et al. (1998), Stojanovic et al. (2000), and Yang (2001). Thus, the optimum calcination temperature can be considered among the lowest compared to that reported the literature. If compared to the calcination temperature required by solid-state reaction, i.e. 850 °C by Gupta et al. (1998) and 950 °C by Barranco et al. (2003), the temperature obtained from this work is approximately one third or even one half lower than those values. This observation could be accounted for by 3 factors:

1. Usually, calcination is effected by providing an external energy from the furnace to the outer surface of the powder. In this case, the heat generated in the exothermic reaction from organic compound decomposition in the particles created an internal energy inside the particle (Das et al., 1998). This energy contributes directly to the formation of crystalline structure. Both energies when added up create a large amount of energy available to facilitate crystalline phase(s) formation and the lowering of the calcination temperature.

2. It is the advantage of coprecipitation method to obtain a homogenous distribution of the constituent ions. This homogeneous distribution which were achieved at the atomic level rather than particulate scale during solution mixing (Stojanovic et al., 2000), reduces the diffusion distance among them which accelerates the monophasic PLZT formation at comparatively low calcination temperatures (Saha & Pramanik, 1997).

3. The size factor, where a fine powder is known to be highly reactive. Higher reactivity of the nano-sized powder tends to form crystalline structure at a lower temperature compared to larger particles due to a surface effect. The size of the powder is shown in the later part of the report.

When the powder was further calcined at 600°C, the intensity of the peaks for both PLZT and possibly PbO become slightly weaker. The decrease in intensity became more obvious at 710°C and 850°C. This indicates that the evaporation of lead oxide in PLZT solid solution causes the amount of PLZT structure to be lowered or perhaps altered. The diffractogram does not show the presence of any other crystalline peak and this indicates that the breakdown products due to PbO volatilization is amorphous in nature and could not be detected by XRD. Another possibility is that the amount of crystalline structure from the remnant LZT components such as $La_2Zr_2TiO_7$ (Stojanovic et al., 2001), $ZrTiO_4$, or La_2O_3 structure is too small to be detected by XRD (Stojanovic et al., 2001).

Figure 3 shows the X-ray diffractogram for the powder synthesized with Method 3, i.e. hydroxide coprecipitation. Apparently similar to precursor powder B, the precursor is totally amorphous. After it was calcined at 600 °C, crystalline peaks are revealed. P2ZT (ICDD 14-31) peaks appear as the primary phase accompanied by some PbO (ICDD 5-0561) and tetragonal PT (40-99) peaks. Crystalline peaks reach their maximum intensity when the powder is calcined at 710 °C. The peaks for minor phase PbO and PT become more obvious as the calcination temperature increases. The intensity becomes lower as the temperature increases further to 850 °C especially for P2ZT phase. More PT peaks are observed probably due to the breakdown of P2ZT phase, although the intensity of PT becomes slightly weaker as well. This might be due to the fact that P2ZT breakdown at higher temperature tends to formed PT structure which is quite disordered and tends to collapse as well. PT is known to be much high-temperature resistant compared to PbO and P2ZT which collapse easily at 850 °C.

From the result, it is observed that up to the maximum calcination temperature of 850 °C, PLZT peaks did not exist at all. In conclusion, this method needs further study in the future work in order to produce the desired PLZT phase.

Equivalent average particle size of powders, which is also called as an estimated spherical diameter (ESD) by Choy & Han (1997) or particle size from specific surface area (SSA) by Kong (2002b), were calculated from the specific surface area measured by the BET method. All the powders produced were assumed to be uniform spheres. The diameter of the particle is taken as the particle size and is calculated from S.G. which refers to specific gravity and SA which refers to specific surface area provided by the multipoint BET analyzer. Equivalent particle size for the precursor powder was calculated from the specific surface area provided by the BET technique. Figure 6 shows a plot of particle size vs. the calcination temperature.

From the BET result, the surface area of sample B was found to be 32.93 m^2/g. The equivalent particle size was then calculated from the specific surface area and density. In order to achieve better accuracy, the S.G. of the precursor powder was used rather than the theoretical density of PLZT compared to work done by Choy & Han (1997). The equivalent particle size of precursor powder is found to be in the nano range viz. 61.32 nm. This result shows that an organometallic coprecipitation method can produce precipitate within a nano-sized range. Overall, it can be seen very clearly that there is a non-linear trend in particle size development. First the particle size of the powders decreases as the temperature increases from room temperature to 400 °C where the lowest particle size is observed (49.73 nm). Then it goes up again until 600 °C before it goes down at 710 °C and then up again at 850 °C. The particle size (calculated from BET measurement) seems to be fluctuating up and down. One of the most important factors is the size of this particle, which is in nano range, which contributes significantly to the measurement of particle size by BET if some form of agglomeration take place. Generally, the higher the temperature, the larger the size is. It is a common fact that, material with a larger surface area (smaller particle size) is much more reactive compared to a material with smaller surface area (larger particle size). As the material with larger surface area (or smaller particle size) is heated to higher temperatures, less energy is required for the material to rearrange the chemical/crystal structure. During the rearrangement of the structure, the surface area tends to be minimized so that the reactivity could be minimized.

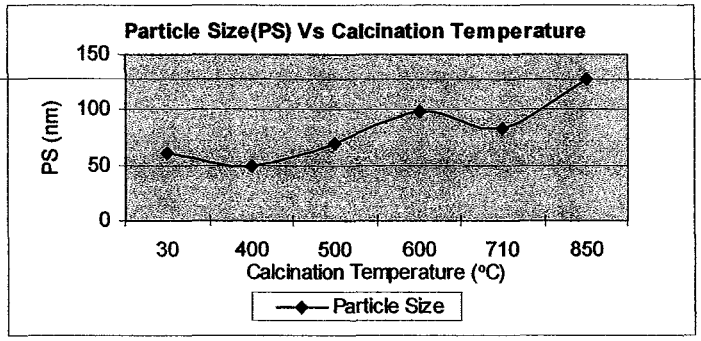

Figure 6: Particle size (PS) for precursor and calcined powders B

Not all wet chemical synthesis promise nano-sized powder such as citrate route (Cerqueira et al., 1998) and solution mixing (Yang et al., 2000). As compared to other methods, the method used in this study gives a satisfactory result by producing powder with dimensions in the nano range of about 50 -130 nm. Compared to a solid-state reaction which reacts the constituents at particulate level, a wet chemical synthesis provides a platform for homogenous mixing of the constituents at atomic scale rather than particulate (Stojanovic et al., 2000).

The precursor powder was then examined with SEM. Figure 7 shows SEM micrographs of the powder before calcination. Apparently, the precursor powder is highly agglomerated. The observed clusters are indicative of agglomeration. There could be 2 reasons for this agglomeration. Firstly, the presence of organic compounds that can bind individual particles together, and secondly the tendency of nano particles to agglomerate to be more stable by minimizing their surface energy. Stojanovic (2001) pointed out that submicron particles can easily agglomerate due to their highly reactive characteristic. The size of this agglomerate is quite large, most of them are larger than 10 μm. Individual particle cannot be seen clearly. As a result, TEM is used with the intention to have a closer look to these particles.

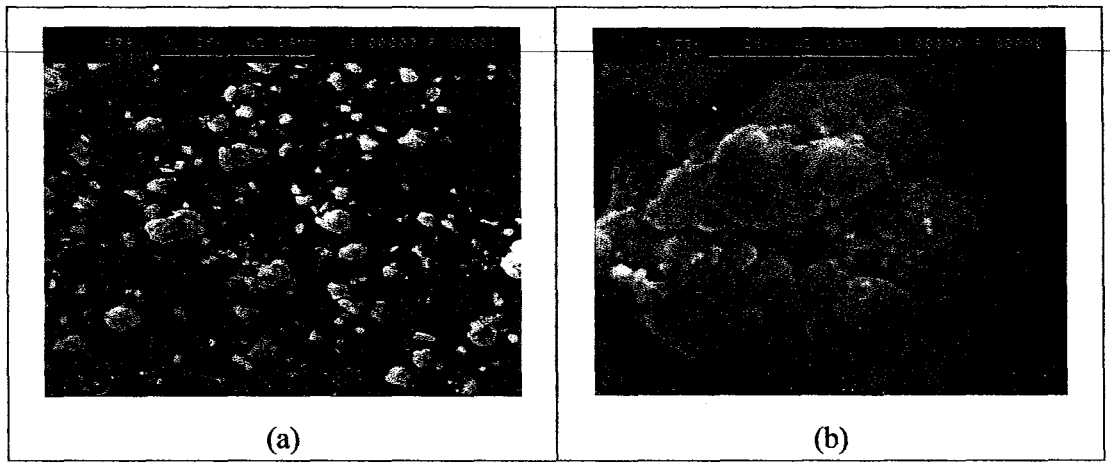

(a) (b)

Figure 7: SEM micrographs of precursor powder before calcination at magnification: (a) 639 times; (b) 4,330 times

TEM was used with the intention to observe the particle clearer. By utilizing TEM, the shapes and sizes of the precursor powder were observed (Figures 8). From the TEM micrographs, it is observed that the shape of precursor powder before calcination is not uniform; this might be due to the fact that a coprecipitation method involves various organic compounds. Size of the agglomerated powder which can be observed was not regular. The agglomeration of precalcine powder is rather severe. As a result, individual particle cannot be imaged; size of the particle cannot be measured too.

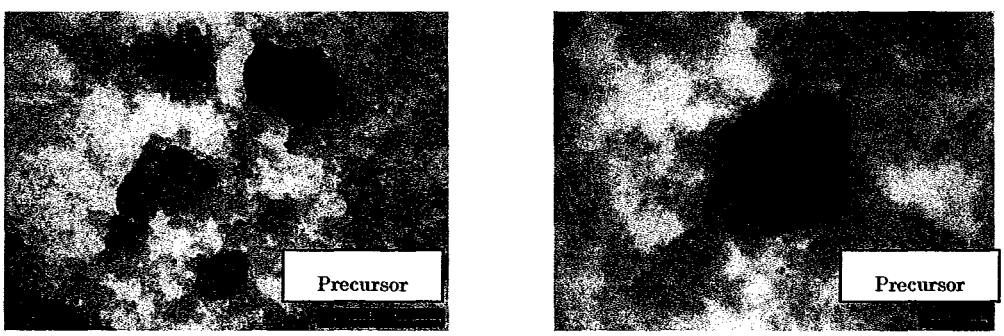

(a) (b)

Figure 8: TEM micrograph of precursor powder B at magnification: (a) 175,000 times; (b) 2,000,000 times

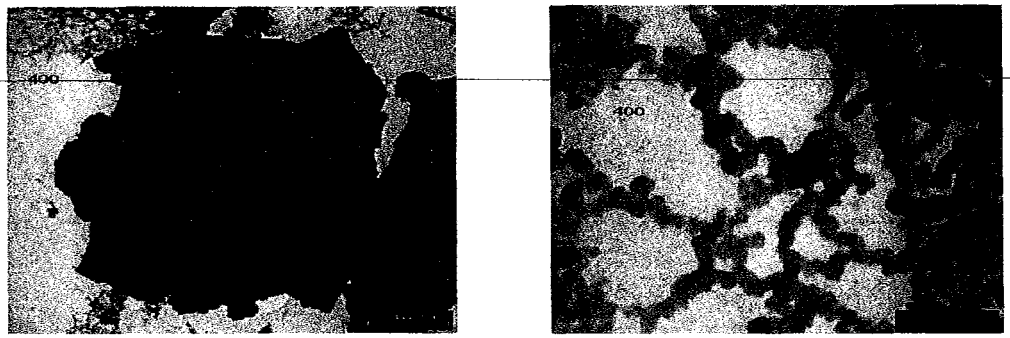

Figure 9: TEM micrograph for B7 powder calcined at 400 °C at magnification: (a) 26,000 times, (b) 320,000 times

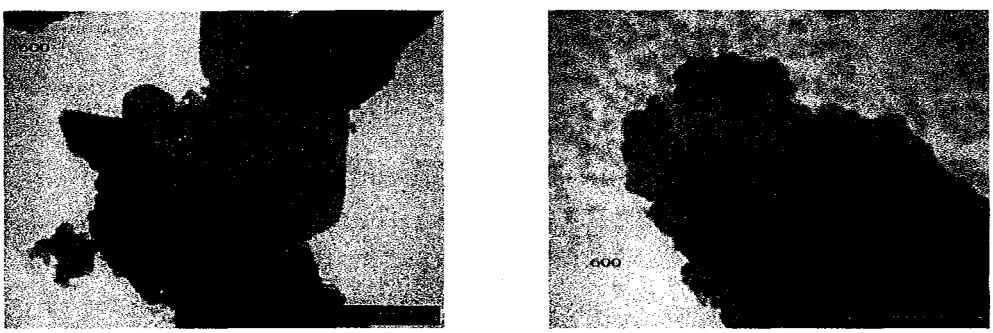

Figure 10: TEM micrograph for B7 powder calcined at 600 °C at magnification: (a) 150 ,000 times; (b) 300,000 times

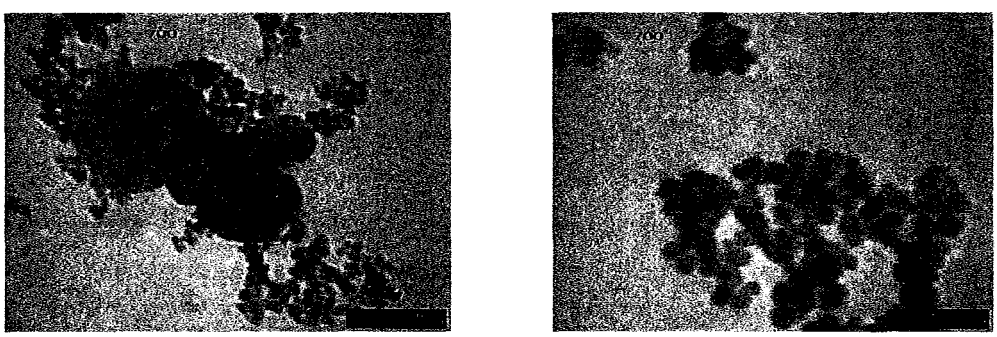

Figure 11: TEM micrograph for B7 powder calcined at 710 °C at magnification: (a) 150 ,000 times; (b) 300,000 times

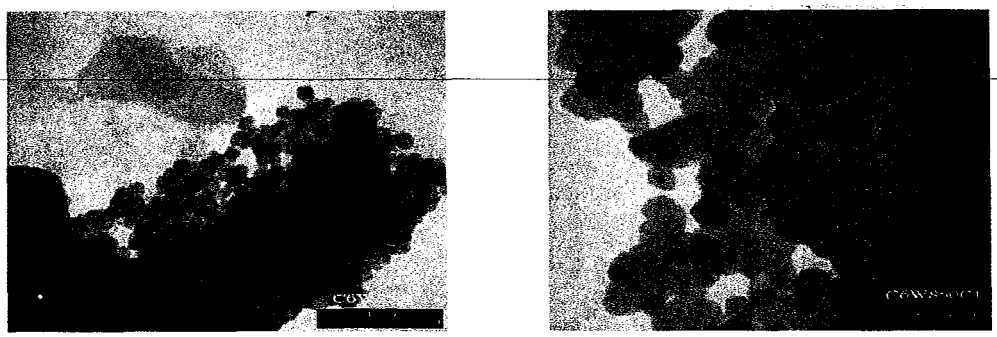

Figure 12: TEM micrograph for B7 powder calcined at 850 °C at magnification: (a) 200,000 times; (b) 400,000 times

Despite particle agglomeration, individual particles for calcined powders could still be observed clearly from the TEM micrograph. Figure 9, Figure 10, Figure 11 and Figure 12 show the TEM micrographs for powders calcined at temperatures 400, 600, 710, and 850 °C respectively.

When the precursor powder was calcined at 400 °C, some of the organic compounds were removed (although some other organics might remain as what is probably shown as large aggregates in Figure 9). In limited places where nano particles are observed to be truly dispersed, the size is much finer. The average particle size for the powder calcined at 400 °C was found to be 10 nm by taking the mean value of the size measured from twenty particles.

The nano particles which are observed in this TEM micrograph is suspected to be the PLZT phase when they are compared to TEM micrograph for powders calcined at some other temperatures (Figures 10-12) where particles with similar sizes and shapes are seen. However, upon referring to the XRD diffractogram for powder calcined at 400 °C (Figure 2), only an amorphous phase is detected. Thus, it is suggested that a PLZT phase has already been formed at 400 °C, but it cannot be detected by XRD due to its amorphous phase or low quantity (probably less than 3 wt.%, Stojanovic et al., 2001) compared to the organic contents as seen in Figure 2. This shows that TEM is also useful in phase identification for phase of material which exists in low quantity.

With an increase in temperature, more organic compounds were eventually liberated and only crystallite PLZT powder should remain. As a result, the percentage of PLZT phases increased. When the powders were calcined at 500-600 °C, the nano particles

were agglomerated (Figures 10) owing to their nature to minimize surface area and energy by forming larger agglomerates which has been discussed in Section 4.4.4. In this temperature range, the particles were seen less dispersed than those calcined at 400°C.

The micrographs for the powder calcined at 710 °C (Figure 11) show that the some of the agglomerates were then broken up when they were calcined at this temperature range. At 850 °C, the particles agglomerate again and this can be observed from both the increase in particle size obtained from surface area and highly "stick-together particles" in the TEM micrographs (Figure 12).

A summary of particle size produced from each calcination temperature is tabulated in Table 2 below and compared to the results of other workers. The particle size analysis as reported by Choy & Han (1997) and Shannigrahi et al. (2000), referred to individual particles without taking agglomeration into account. From the TEM micrographs shown by Choy & Han (1997), agglomeration could be observed as well. The degree of agglomeration could not be determined since the scale was not given. Micrographs shown by Shannigrahi et al. (2000) was much well dispersed compared to the powder produced in this work and that by Choy & Han (1997). This could be attributed to the technique used for dispersion which could be further improved.

Table 2: Comparison of PLZT particle size synthesized by various methods

Author	Year	Method	Particle Size	Remark
Choy & Han	1997	Citrate Route	30 nm	Wet chemical synthesis
Cerqueira et al.	1998	Pechini & Partial Oxalate	SSA: 2.31-5.86 g/cm^3 Estimated particle size (not given): > 150 nm	Wet chemical synthesis
Yang	2001	Solution Mixing	770 nm (Mean) 930 nm (Median)	Wet chemical synthesis * Size obtained by laser particle size analyzer
Kong et al.	2002	Ball Mill	250 nm (4 Hr) 158 nm (15 Hr) 176 nm (36 Hr)	Mechanical activation solid state reaction
Yeoh et al. (Present work)	2004	Organometallic Coprecipitation	SSA: 23.66-6.67 g/cm^3 PS: 49 – 129 nm	Wet chemical synthesis

The calcined powder B was then pressed into pellets and sintered in 2 different atmospheres, i.e. PbO-rich and ambient, at 1200°C, 1250°C and 1300°C, based on results suggested from dilatometric tests. After being sintered, the pellets were coated with Ag-Pd before dielectric measurements were carried out. Dielectric constant at 10 KHz for each sample was made, and the capacitance characteristics of the samples sintered in PbO-rich atmosphere and in ambient atmosphere are shown in Figure 13 and Figure 14, respectively. Overall, the samples sintered in PbO-rich atmosphere show higher dielectric constants (max 1770±1). This could be attributed to the low density of the samples sintered in ambient atmosphere as well as the evaporation of PbO in the PLZT framework that leads to the formation of a secondary phase. Generally, the dielectric constant measured from the samples obtained by this method are considered to be acceptably high (Yang, 2001, Zhang et al., 2003).

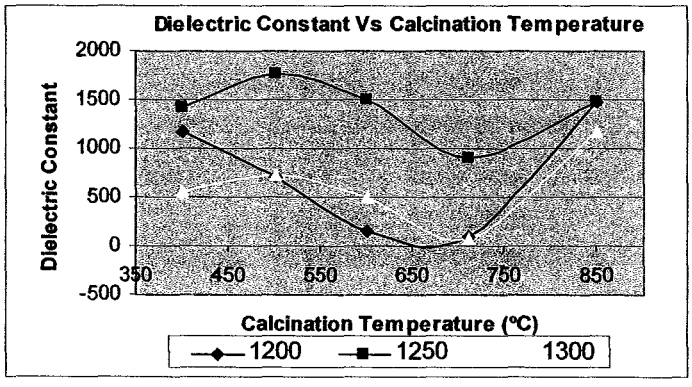

Figure 13 : Dielectric constant of samples sintered in a PbO-rich atmosphere

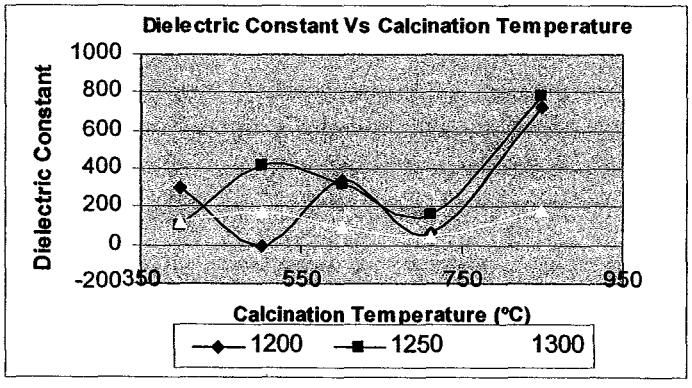

Figure 14 : Dielectric constant of samples sintered in an ambient atmosphere

Conclusions

Nano-crystalline PLZT powder has been successfully synthesized by the present novel coprecipitation method. The sizes of the powders can be controlled to be within the nano-size range whilst a high dielectric constant is also obtained (which is a good ferroelectric property).

Research Output

This project has successfully produced an M.Sc. student. Besides, a few papers listed below were also published on this project.

1. F.-Y. Yeoh (2003).
   Synthesis And Characterization Of Nano-Sized PLZT Powder Derived From A Modified Coprecipitation Method (Master Thesis), Seri Ampangan: Universiti Sains Malaysia (USM).

2. F.Y. Yeoh, A. Aziz, A. and R. Othman (2003).
   Thermal Behaviour of Coprecipitation-Derived PLZT, *Proceeding of 3rd International Conference on Recent Advances in Materials, Minerals and Environment (RAMM 2003)*, p. 364, 20 – 22 Oct 2003, Penang, Malaysia.

3. F.Y. Yeoh, R. Othman, and A. Aziz (2002).
   Synthesis and characterisation of ferroelectric PLZT material using x-ray diffractometry, *Malaysia Journal of Science*; **21A**, 77-81.

4. F. Yeoh, R. Othman and A. Aziz. (2002). Preparation of Nano Cystalline Lead Zirconate Titanate and Lead Lanthanum Zirconate Titanate Powder; *Postgraduate Research Paper 2001-2002*; **1**, 29-30, Seri Ampangan: Universiti Sains Malaysia (USM).

Acknowledgement

A grant from Nippon Sheet Glass Foundation which has made this research work possible is gratefully acknowledged.

References

Barranco, A.P., Tera, A.H., Monjaras, R.V., Eiras, J.A., Garcia, D., Pinar, F.C. & Martinez, O.P. (2003). Influence of synthesis process on the ac response of PLZT (8/65/35) ferroelectric ceramics. *J. Euro. Ceram. Soc.* **23**, 1337-1343.

Cerqueira, M., Nasar, R.S., Leite, E.R., Longo, E. & Varela, J.A. (1998). Synthesis and characterization of PLZT (9/65/35) by he Pechini method and partial oxalate. *Mater. Lett.* **35**, 166-171

Choy, J. H. & Han, Y.S. (1997). Citrate route to the preparation of nanometer size (Pb, La)(Zr, Ti)O_3 oxide. *Mater. Lett.* **32**, 209-215.

Das, R.N., Pathak, A. & Pramanik, P. (1998). Low-temperature preparatipon of nanocrystalline lead zirconate titanate and lead lanthanum zirconate titanate powders using triethanolamine. *J. Am. Ceram. Soc.*, **81** (12), 3357-3360.

Gupta, S.M., Li, J.F. & Viehland, D. (1998). Coexistence of relaxor and normal ferroelectric phases morphotropic phase boundary compositions of lanthanum-modified lead zirconate titanate. *J. Am. Ceram. Soc.* **81**(3), 557-564.

Kong, L.B., Ma, J., Zhu, W. & Tan, O.K. (2002b). Preparation and characterization of PLZT (8/65/35) ceramics via reaction sintering from ball milled powder. *Mater. Lett.* **52**, 378-387.

Potdar, H.S., Deshpande, S.B. & Date, S.K. (1994). Synthesis of PLZT powders via a molecularly modified precursor route. *Mater. Lett.* **19**, 269-274.

Saha, S.K. & Pramanik, P. (1997). Synthesis of nanophase PLZT (12/40/60) powder by PVA-solution technique. *Nanostructured Material.* **8** (1), 29-36.

Shannigrahi, S.R., Choudry, R.N.P., Achrya, H.N. & Sinha, T.P. (2000). Microstructure and electrical characterizations of K-modified PLZT. *J. Mat. Sci.* **35**, 1737-1742.

Stojanovic, B.D., Zaghete, M.A., Paiva-Santos, C.O., Cilense, M., Magnano, R., Longo, E. & Varela, J.A. (2000). Hot-pressed 9.5/65/35 PLZT prepared by the polymeric precursor method. *Ceram. Int.* **26**, 625-630

Stojanovic, B.D., Foschini, C.R., Cilense, M., Zaghete, M.A., Cavalheiro, A.A., Paiva-Santos, C.O., Longo, E. & Varela, J.A. (2001). Structural characterization of organometallic-derived 9.5/65/35 PLZT ceramics. *Materials Chemistry and Physics.* **68**, 136-141.

Yang, W.D. (2001) PZT/PLZT ceramics prepared by hydrolysis and condensation of acetate precursors. *Ceram. Int.,* **27**, 373-384.

Zhang, Y., Ding, A.L., Qiu, P.S., He, X.Y., Zheng, X.S., Zeng, H.R. & Yin, Q.R. (2003). Effect of La content on characterization of PLZT ceramics. *Mat. Sci. & Eng. B.*, **99**, 360-362.